

## DISTRIBUTION AND PROPAGATION MECHANISMS OF PD PULSES FOR UHF AND TRADITIONAL ELECTRICAL MEASUREMENTS

S.M. Hoek<sup>1\*</sup>, M. Koch<sup>1</sup> and M. Heindl<sup>2</sup>

<sup>1</sup>OMICRON electronics GmbH, Oberes Ried 1, 6833 Klaus, Austria

<sup>2</sup>Universität Stuttgart, Pfaffenwaldring 47, 70569 Stuttgart, Germany

\*Email: stefan.hoek@omicron.at

**Abstract:** Partial Discharge (PD) measurements are considered as a very powerful technique for testing and monitoring the condition of high-voltage (HV) insulations. PD diagnostics is generally accepted as an early breakdown indicator, which is also reflected in numerous standards. In the present contribution, the authors describe the fundamentally different propagation mechanisms of electrical impulses in the conventional (according IEC 60270) and the ultra high frequency (UHF) range. The low frequency components of the PD signals propagate mainly via the conductor whereas the high frequency components (UHF signals) are radiated as electromagnetic waves. The sensitivity and spectrum of the measurement depends strongly on the geometric position of the PD, damping and resonances of the propagation path and the frequency response of the receiver. Field simulation has been used as an appropriate tool for calculating PD signal propagation in HV apparatus.

### 1 INTRODUCTION

An important and worldwide accepted element for quality control of HV insulation systems is the PD measurement [1]. Partial discharges are local electrical discharges that partially break down the HV insulation [2] and generate electric impulses as well as electromagnetic waves in a broad frequency spectrum due to their short rise time and duration [3]. Rise times from PD signals of protrusions down to 35 ps, corresponding to frequencies up to 10 GHz, have been verified [4]. Measurement and detection of PD is performed with different methods involving different propagation paths, propagation mechanisms and sensor principles which result in divergent transfer behavior. The measurable signal spectrum (magnitude vs. frequency) depends directly on source geometry and location, structure of the test setup and the used sensor and measurement technology. Figure 1 illustrates the propagation of PD signals from source to receiver. The originally very wide frequency spectrum of the Dirac-like discharge spark is modified by the electric characteristics of its close surroundings, the propagation path with its damping and resonances and finally by the frequency response of the measurement system.

Traditional setup according to IEC 60270 uses band pass filters in the range of some 100 kHz, aiming to measure in a frequency range less subject to external disturbances which are typically radiating in a broad frequency spectrum. For higher centre frequencies of some 100 MHz, a fundamentally different nature of the disturbances can be expected; having often more narrowband character. However, PD pulses with their broadband spectral energy will radiate in the lower

frequency range as well as in this UHF range [5][6].

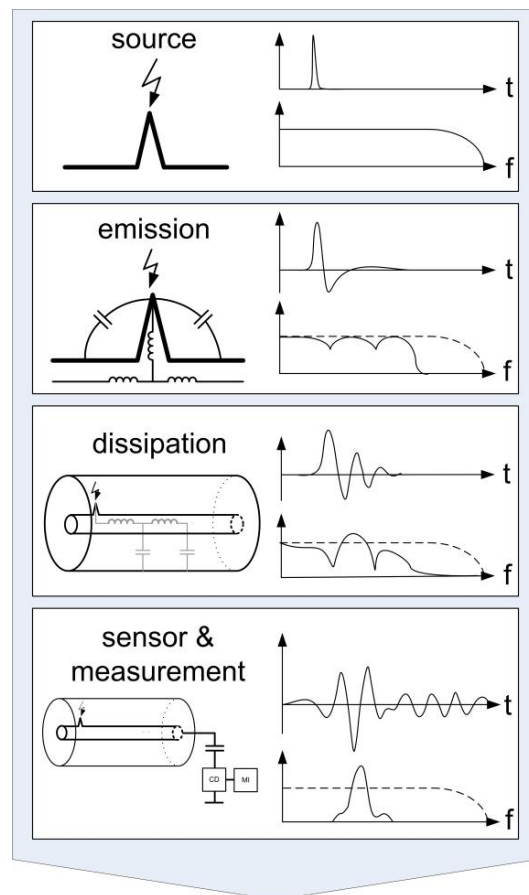


**Figure 1:** PD signal propagation and variation in frequency spectrum from source to test system.

By choosing a suitable measurement frequency range or by combining of both, the conventional

and the UHF technique, external disturbances can be handled much better. This different behaviour of disturbances and PD pulses and the different sensor principle lead to some advantages for the UHF method e.g. avoid corona disturbances during on-site measurements. However there are general uncertainties related to the comparability of the UHF measurements to conventional IEC conformant tests [7]. For example, during Cigré Session 2008 the Special Reporter of SC D1 asked the question: "How can the relation between the conventional PD measurement and the UHF measurement determined and generalized?" [8].

In the present contribution, the authors detail the fundamentally different propagation mechanisms of electric impulses based on Maxwell's law of total current. Simulation results of PD signal propagation in gas-insulated switchgear (GIS) illustrate graphically the complex and very geometry sensitive transfer function of UHF signals. The authors conclude that a general correlation between conventional PD measurements and these in the UHF range does not exist.

According to the IEC 60270 standard (conventional method), the PD signals are measured with a coupling capacitor ( $C_k$ ) and coupling device (CD) (Figure 2 / right). With the UHF method, the PD signals are detected in the UHF frequency range with disk couplers or other antennas (Figure 2 / middle).

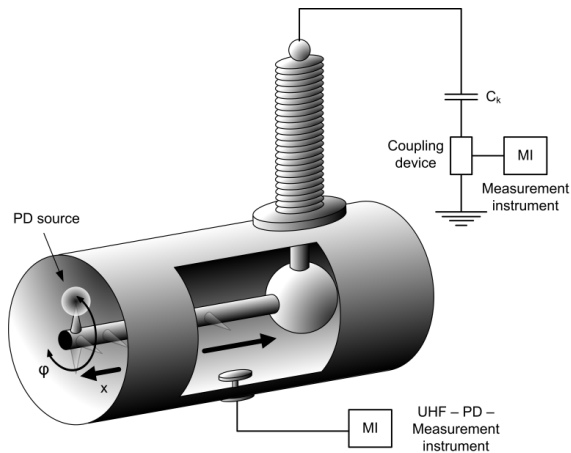


**Figure 2:** Detection of PD sources in GIS by conventional and UHF method.

## 2 THEORIE OF IMPULSE PROPAGATION

### 2.1 Maxwell's Law of Total Currents

For describing the principles of electro-magnetic impulse propagation, one may start with the famous equations of Maxwell. An electrical field  $E(t)$  generates a current density  $J(t)$  as a sum of conduction and displacement currents, where  $\sigma_0$  is the volume conductivity of that material. From (1) it can be concluded that

- Electrical conduction consists of two phenomena, where one is related to a conductor and the other to an insulating medium existing between the conductors.

- The second phenomenon, displacement current, is particularly present for fast variations of  $d/dt$ , that is for high frequencies and leads to electromagnetic wave propagation.

$$\nabla \times H(t) = J(t) = \sigma_0 E(t) + \frac{dD(t)}{dt} \quad (1)$$

### 2.2 Signal Propagation for Low Frequencies

The propagation of PD signals with low frequencies in conductors usually takes place by conduction currents. In a conductor, the surrounding magnetic field is closed. The electric field has its origin on the conductor surface and spreads radially. Neither H-field nor E-field have components in the direction of propagation. This corresponds to the definition of propagation of the TEM-mode, able to propagate from DC to very high frequencies.

### 2.3 Electro-Magnetic Wave Propagation

For these higher frequencies the conductive structure works increasingly as an antenna, which cut-off frequency depends on the dimensions especially close around the PD source. Correspondingly, the structure of the PD source influences the PD signal.

The transfer function is significantly influenced by resonances. These are caused by the capacitance and inductance of the propagation path. The wavelengths of the PD signals are of the same order as the physical dimensions of the GIS, while the nominally coaxial signal path of the GIS exhibits many discontinuities which lead to complex resonance patterns of electromagnetic waves within each compartment.

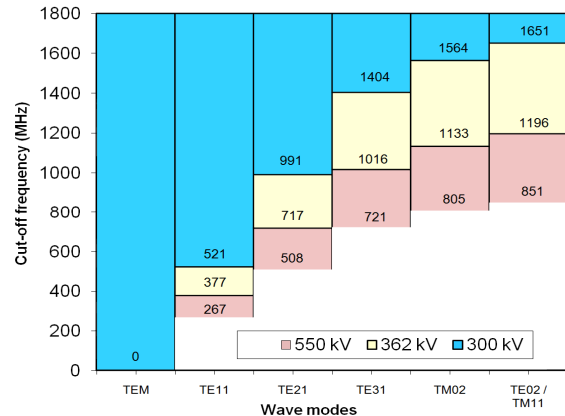


**Figure 3:** Cut-off frequencies ( $f_c$ ) within a GIS for 300 kV, 362 kV and 550 kV [9]

Additionally to the basic TEM signal propagation mode, higher order modes (TE- and TM-mode) may propagate depending on the geometry. The higher order modes propagate only above their cut-off frequencies ( $f_c$ ). In Figure 3 the cut-off frequencies of the first wave modes are shown for three different diameters, respectively different types of GIS.

Each of this higher order modes are reflected at discontinuities, generate interference patterns and standing waves (resonances), and are damped by skin effect and lossy dielectric material. What is finally picked up at the broadband UHF PD sensor (built into the GIS) is the complex superposition of all modes, which result in a frequency spectrum with various resonances and frequency bands with highly different measurement sensitivity.

In the terminology of the high frequency technique, the GIS can be described as a heavily overmoded waveguide [10].

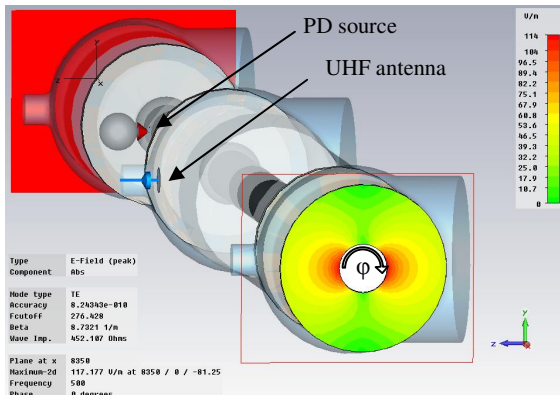


**Figure 4:** Electrical field distribution of  $TE_{11}$  wave mode inside GIS

The TE- and TM-mode (often called higher modes) have H- and E-field components in the propagation direction and show in the transversal plain an un-symmetrical field distribution (Figure 5) [11]. This field distribution explains the transmission of the PD signal from source to sensor as a function of the angle  $\varphi$  between source position in relation to the sensor position.

The analysis of the energy distribution of the different modes over the frequency range is shown in Figure 5. It reflects the importance of the higher modes for the signal propagation in the UHF range.

Due to the skin effect and losses at spacers the propagating signals are damped; these effects are frequency dependent.

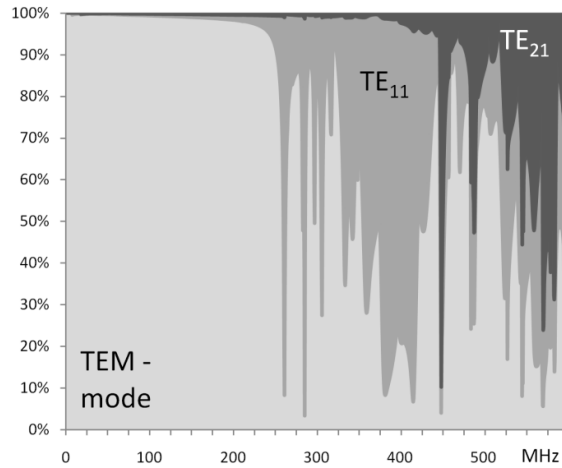


**Figure 5:** Share of the TEM-wave modes and higher modes ( $TE_{11}$  and  $TE_{21}$ ) at the total transfer versus the frequency [12]

The complexity is further increased by considering the frequency dependence of the group velocity ( $v_g$ ) of the TE- / TM-wave modes especially around their cut-off-frequency [9].

$$v_g(f) = c_0 \cdot \sqrt{1 - \left(\frac{f_c}{f}\right)^2} = \sqrt{1 - \left(\frac{f_c}{f}\right)^2} / (\epsilon_0 \cdot \mu_0) \quad (2)$$

These shown transfer mechanisms sum up to a complex spectrum which is measurable at the UHF sensors.

### 3 SIMULATION OF PD SIGNAL PROPAGATION IN GIS

#### 3.1 Simulation Model

In order to investigate characteristics of the two common PD measurement principles, a simulation model of a GIS was created using CST Microwave Studio (MWS) software package. MWS uses finite integration technique (FIT) to solve electromagnetic field problems in time domain [13]. It is suitable to simulate electromagnetic wave propagation mechanisms through air and wire within electrically large structures like GIS. Figure 6 shows an overview of the simulation arrangement. The model consists of an evacuated tube of 7.4 m length with diameter of 55 cm and a centred inner conductor tube with 16 cm diameter. The inner conductor is held in position by three epoxy resin spacers (assumed  $\epsilon_r = 4.0$ ). Both ends of the GIS are terminated with so-called waveguide ports which are adapted to the characteristic wave impedance of the arrangement. This technique provides absorption of wave energy and inhibits total reflection at both ends of the structure. Otherwise reflections would keep electromagnetic waves propagating through the lossless arrangement over and over again without decreasing of

the overall field energy, which would be an unrealistic boundary condition.

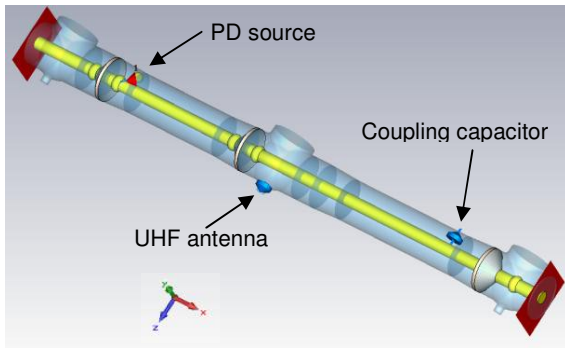


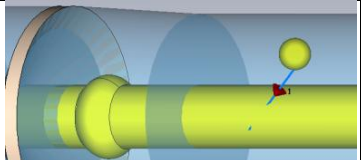
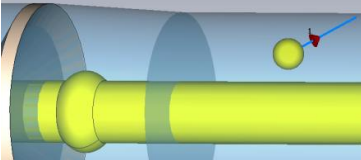
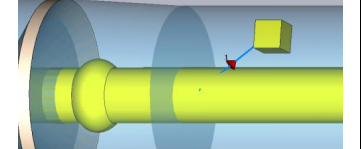
**Figure 6:** GIS model overview in CST MWS

The injection of PD pulses into the inner conductor of the GIS, i.e. simulation of a PD source, was carried out by an additional insulated spherical structure respectively cubical conductor between the inner and outer conductor (Table 1). A pulse voltage source connects the sphere or cube to the GIS. This composition fulfills two purposes:

- Radiation of electromagnetic waves as they are caused by real PD sources
- Injection of a “PD current” into the conducting part of the GIS

As described above, decoupling of the PD signals is done in two different ways. Firstly, a coupling capacitor (referred to as coupling device, CD, Figure 2) provides monitoring of line coupled signals according the IEC arrangement. Both for the conventional CD and the UHF antenna, PD signals can be recorded by monitoring voltage and current through lumped elements.

**Table 1:** PD Source Configurations

Type		PD Source Configuration
1		Spherical Shape, Inner Conductor Fed
2		Spherical Shape, Outer Conductor Fed
3		Cubical Shape, Inner Conductor Fed

### 3.2 Simulation Results

The first experiment simulates a PD event using the spherical structure described above as PD source (Table 1/Type 1). The position of the PD source is defined by its x-position and angle within the yz-plane (Figure 2). First the x-position of the PD source was varied while the angle  $\phi$  was constant; second the angle was varied while the x-position was constant (Figure 2). Figure 7 shows the measurable UHF antenna peak voltage and apparent charge level when the x-position was varied.

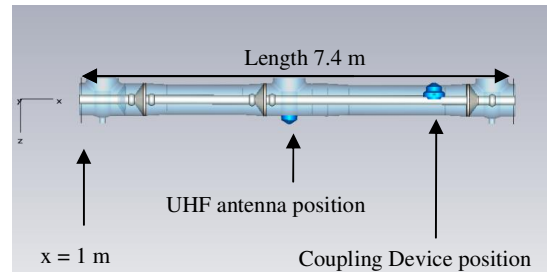
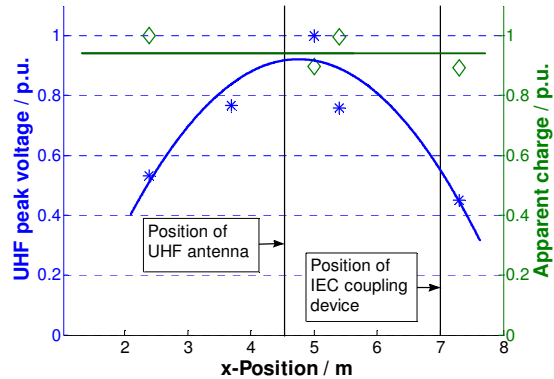


**Figure 7:** UHF peak voltage and apparent charge level vs. position of simulated PD source

Signal damping clearly increases with distance between UHF antenna (fixed position) and PD source. The apparent charge level shows only minor sensitivity to the position of the PD, due to resistive and inductive damping. Figure 8 shows apparent charge level and peak voltage picked up by the UHF antenna when the x-position of the PD source was kept constant and its angle  $\phi$  was varied in steps of 90°. Again, the apparent charge level remains almost constant while the UHF peak voltage varies by almost 25%. This can be explained by the complex wave propagation mechanisms for signals in the UHF range [12].

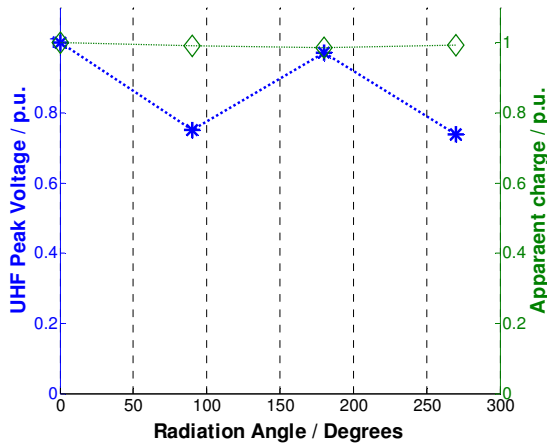


**Figure 8:** UHF peak voltage and apparent charge level vs. radiation angle of PD source

This effect is explainable by wave modes inside of the GIS. The field components in the direction of propagation of the TE- / TM-modes results in a angel dependence of the field distribution in the yz-plane as it is shown in Figure 4.

In further experiment simulates the PD source is modified, in the following way. The diameter of the PD source was decreased form 60 mm (like Table 1/type 1) to 30 mm while the position of the sphere is constant. Figure 9 shows the measurable UHF antenna peak voltage and apparent charge level when the diameter was varied.

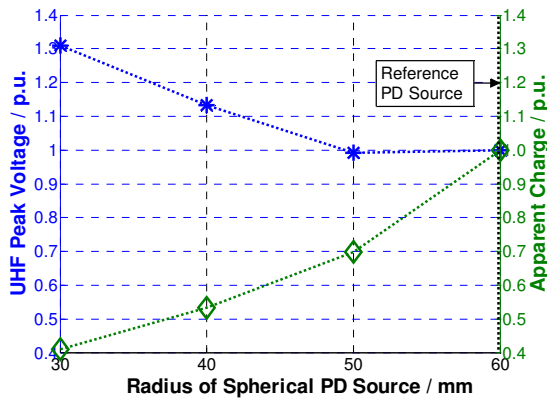


**Figure 9:** UHF peak voltage and apparent charge level vs. size PD source

Due to smaller clearances between PD source and conduction structure for enlarged radius the capacitive coupling is increased. This leads to an increasing apparent charge level for extended radiuses. In contrast to that the UHF peak voltage decreases for bigger sphere diameters, which can be explained by changed radiation characteristics.

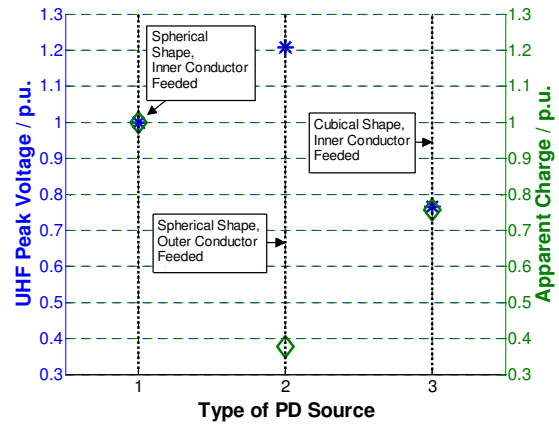


**Figure 10:** UHF peak voltage and apparent charge level vs. different PD source (Table 1)

Figure 10 shows the measurable UHF antenna peak voltage and apparent charge level when the source shape type was varied according to Table 1. Both UHF antenna peak voltage and apparent charge level was normalised on source type 1.

The capacitance between sphere and outer conductor (type 1) is higher than the capacitance between sphere and inner conductor (type 2). Due to this also the apparent charge level is reduced for source type 2. In contrast to that the UHF antenna peak voltage is increased by the changed radiation characteristics. For PD source type 3 the circumstances are comparable to source type 1 which gives a corresponding UHF and apparent charge level.

#### 4 CONCLUSIONS

- The low frequency components of the PD signals propagate mainly via the conductor. It is expected that in large setups, the damping of the signal is not negligible during calibration and measurement.
- The high frequency components (UHF signals) propagate through electromagnetic waves. The propagation is mainly influenced by the geometric circumstances.
- The sensitivity of the UHF measurement and its spectrum depends strongly on the geometric position of the PD, geometry of the source, damping and resonances of the propagation path and the frequency response of the receiver.
- Field simulation has been used as an appropriate tool for calculating PD signal propagation in HV apparatus.

UHF antenna peak voltage and apparent charge level cannot be compared directly in our simulation setup. While the measureable apparent charge

level of PD sources is mainly determined by the capacitive couplings of the structures and the conductor properties, the detectable UHF signal is influenced by the geometry of the GIS and source.

## 5 REFERENCES

- [1] D. König and Y.N. Rao: "Partial Discharges in Electrical Power Apparatus", VDE 1993
- [2] IEC 60270, "High-voltage test techniques – Partial discharge measurement", Version 2000, 3rd Edition
- [3] M.D. Judd, S. Meijer and S. Tenbohlen, "Sensitivity check for RF PD detection for power transformers," IEEE Conference on Condition Monitoring and Diagnosis (CMD), Peking, China, April 21-24, 2008, paper No. K1-03
- [4] A.J. Reid, M.D. Judd; "High Bandwidth measurement of Partial Discharge Pulses in SF<sub>6</sub>"; 14th ISH Beijing, China, August 25-29 2005; G-012
- [5] M.D. Judd, O. Farish, B.F. Hampton, "The Excitation of UHF Signals by Partial Discharges in GIS", IEEE Transactions on Dielectrics and Electrical Insulation, Vol. 3 No. 2, April 1996
- [6] S. Tenbohlen, S.M. Hoek, D. Denissov, S.M. Markalous, "Partial Discharge Measurement in the Ultra High Frequency (UHF) Range," IEEE Tr. on Dielectrics and Electrical Insulation, Vol. 15, No. 6/2008, pp. 1544-1552
- [7] S.M. Hoek, S. Coenen, M. Bornowski, S. Tenbohlen: "Fundamental Differences of the PD Measurement according to IEC 60270 and in UHF range", 2008 International Conference on Condition Monitoring and Diagnosis, Beijing, China, April 21-24, 2008
- [8] J. Densley et al. "Special Report for Group D1", Cigré Main Session 2008, online available at [www.cigre.org](http://www.cigre.org)
- [9] S.M. Hoek, U. Riechert, T. Strehl, K. Feser, and S. Tenbohlen, "New Procedures for Partial Discharge Localization in Gas-Insulated Switchgears in Frequency and Time Domain", ISH Ljubljana / Slovenia, August 2007
- [10] S.M. Hoek, S.M. Neuhold, "Tuned Medium-Band UHF PD Measurement system for GIS" 17<sup>th</sup> ISH Hannover, Germany, August 2011
- [11] R. Kurrer, K. Feser, "The Application of Ultra-High-Frequency Partial Discharge Measurements to Gas-Insulated Substations", IEEE Transactions on Power Delivery, Vol. 13, No. 3, July 1998
- [12] S.M. Hoek, M. Koch and M. Heindl, "Propagation Mechanisms of PD Pulses for UHF and Traditional Electrical Measurements" IEEE Conference on Condition Monitoring and Diagnosis (CMD), Tokyo, Japan, Sept 06-11, 2010, paper No. C2-02
- [13] I. Munteanu, M. Timm, T. Weiland, "It's About Time," Microwave Magazine, IEEE, vol. 11, issue 2, pp. 60–69, March 2010.